Composites Part B 238 (2022) 109901

Contents lists available at ScienceDirect

Composites Part B

journal homepage: www.elsevier.com/locate/compositesb

Sustainable plastic composites by polylactic acid-starch blends and bleached kraft hardwood fibers

Ferran Serra-Parareda [a], Marc Delgado-Aguilar [a], Francesc X. Espinach [a], Pere Mutjé [a,b], Sami Boufi [c], Quim Tarrés [a,b,*]

[a] LEPAMAP-PRODIS Research Group, University of Girona, Maria Aurèlia Capmany, 61, 17003, Girona, Spain
[b] Chair on Sustainable Industrial Processes, University of Girona, Maria Aurèlia Capmany, 61, 17003, Girona, Spain
[c] University of Sfax, Faculty of Science, LMSE, BP 802-3018, Sfax, Tunisia

ARTICLE INFO

Keywords:
Green composite
Biobased polymer blends
Natural fibers
Sustainable materials

ABSTRACT

The growing environmental consciousness of society has led to the development of sustainable products. Because of its noticeable tensile properties, polylactic acid (PLA) has been widely studied as a replacement for non-degradable and renewable polymers. However, the PLA by itself has a high rigidity that is increased when fibers are incorporated as reinforcement. In this sense, the present work aims to study the feasibility of obtaining compounds with high properties while maintaining a lower stiffness. For this purpose, a mixed PLA-PTA (thermoplastic starch-based polymer) matrix was chosen. The use of PTA to increase the compostability of the material caused the tensile strength decrease of 37.3%, the Young's modulus reduction of 34.9% and the strain decrease of 12.6% compared to PLA matrix when 30% PTA was added. Therefore, blends were reinforced with bleached kraft hardwood fibers (BKHF) to improve their mechanical performance. In the case of the blend with 20% PTA reinforced with 30% BKHF, 51.32 MPa tensile strength (35.4% of increase), 5.54 GPa Young's modulus (112.3% of increment) and a strain of 4% (23.5% of gain). Thermal, morphological and macro-mechanical properties of blends were investigated. It was found that the tensile properties and the interphase of the two components were fairly good in comparison with the literature. The study has allowed us to conclude through a preliminary LCA that it is possible to obtain materials with the same properties of PP with a 33.6% reduction in the carbon footprint. Thus, BKHF reinforced biocomposites are postulated as a real alternative to replace non-renewable ones.

1. Introduction

Society's concern about global problems associated with environmental factors has awakened the interest of the scientific community in the use of renewable resources. In this regard, current plastics are receiving much attention, due to their fossil origin and the problems associated with waste management and pollution [1,2]. It is estimated that the current uncontrolled use of plastics could lead to an estimated 12 billion metric tons of plastic waste by 2050 [3]. The environmental problems caused by the consumption of plastics are a global concern and it is for this reason that bio-based and biodegradable materials must be found to provide a solution to this problem [4]. The use of biodegradable polymers such as poly (butylene succinate) (PBS) [5], poly (3-hydroxybutyrate) (PHB) [6], thermoplastic starch (PTA) [7] or poly (lactic acid) (PLA) [8] is focusing research in this field. However, in most cases, bio-based and biodegradable polymers are more expensive than fossil-based polymers and present significant technical difficulties due to either low mechanical properties or excessive brittleness [9,10].

In the case of polymeric matrices, obtaining better mechanical properties is possible by reinforcing them with a fibrous material. A clear example of such materials is glass fiber (GF) reinforced polyolefin [11]. These composites are nowadays commodities largely used in the automotive industry, product design, and aeronautics [12]. The mechanical advantages of materials such GF reinforced polypropylene composites are evident, obtaining tensile and flexural strengths, and moduli noticeably higher than the pure matrices [13,14]. Nevertheless, these materials involve the manipulation of GF, a harmful material, both for the human and the machinery [15]. Additionally, PP involves environmental disadvantages since it is non-biobased and non-degradable, and a high amount of energy is needed to manufacture

* Corresponding author. LEPAMAP-PRODIS Research group, University of Girona, Maria Aurèlia Capmany, 61, 17003, Girona, Spain.
E-mail address: joaquimagusti.tarres@udg.edu (Q. Tarrés).

https://doi.org/10.1016/j.compositesb.2022.109901
Received 16 August 2021; Received in revised form 11 March 2022; Accepted 11 April 2022
Available online 29 April 2022

GF [16]. More specifically, PLA and thermoplastic starch (TPS) blends have been the subject of great interest to reduce the cost of the PLA material and enhance the biodegradability promoted by the presence of starch. A recent review have reported the most progress achieved in this area [17].

The literature shows increasing efforts to find reinforcements able to substitute GF in the shape of lignocellulosic fibers (LCF) [18,19]. Unlike GF, LCF comes from renewable sources and does not present any danger for humans [20]. LCF are less abrasive than GF and does not submit the equipment to attrition [21]. Anyway, LCF presents also some drawbacks as polyolefin reinforcement due to its hydrophilic nature, which is opposed to the hydrophobicity of the matrices [22,23]. These issues have called the attention of the researchers and some solutions, like fiber treatments or the use of coupling agents, have been proposed [24,25]. Notwithstanding, LCF reinforced polyolefins show some drawbacks when are analyzed under mechanical properties, costs, and environmental criteria. While these composites show competitive mechanical properties and costs, the use of oil-based matrices and the need for additional reactants depreciates its sustainability and contradicts some of the principles of green chemistry [26].

PLA, produced by polycondensation of lactic acid, has attracted increasing attention due to its higher mechanical properties than polymers such as polypropylene or polyethylene and its biodegradability, biocompatibility, and non-toxicity [8,27]. Moreover, the costly production process, its intrinsic fragile behavior, low tenacity, and slow biodegradation have limited its implementation [28,29]. In this context, blending PLA with other polymers is an interesting approach to overcome these obstacles. The use of a polymer with superior performance in the areas in which PLA has limitations will make it possible to obtain a material with a compensated performance [29,30]. Thermoplastic starch-based polymers (PTA) are another bio-based and biodegradable materials that have attracted the interest of researchers and the market [31,32]. Nonetheless, they have some deficiencies as well, since their properties are considerably lower than PLA or PP, their processability is poor, and are sensitive to water [33]. This study will present the development of PLA and thermoplastic starch blends as a bio-based and biodegradable material alternative to traditional petroleum-based polymers. Blends of PLA and PTA combine the advantages of two polymers by maintaining biodegradability and improving the properties of PTA. The development of PLA blends may allow the expansion of PLA applications in areas of consumer products where, mainly, the rigidity of this bioplastic has limited it [34].

In this sense, the literature also shows the suitability of PLA to be reinforced with LCF with noticeable mechanical properties comparable to GF-reinforced PP [35,36]. Hence, LCF reinforced PLA composites are promising materials in terms of mechanical performance. Moreover, these composites do not need any coupling agent to obtain quite good interphases. Presumably, such composites are also more sustainable than oil-based composites, but a life cycle analysis is needed to properly sustain this assertion [21]. Also, reinforcing PTA with natural fibers is possible, obtaining fairly good interfaces without any coupling agent [37]. Thus, these composites show cost and presumably environmental advantages, but lower mechanical properties.

Undoubtedly, composite materials are not limited to two phases, and hybrid materials can be formulated and obtained to profit from the better properties of every phase and equalize its drawbacks [38–40]. Hybrid materials add more complexity to the structure of composite materials and ensuring the compatibility between the phases is of utmost importance. The literature shows that PLA or PTA can be reinforced with LCF obtaining good compatibility and improved mechanical properties [41]. Thus, a measured blend of PLA and PTA can lead to materials with competitive mechanical properties. Furthermore, inasmuch as both matrices can be reinforced with LCF, a PLA/PTA blend is expected to be compatible with such reinforcements.

A variety of LCF's, from wood fibers to annual plants or agroforestry waste, can be used as reinforcement of plastics [18,19,42,43]. Nonetheless, such natural reinforcements showed noticeable differences in its intrinsic properties and even fibers from the same species showed large standard deviations from the mean values of such mechanical properties. This property indetermination, in front of glass fibers with traceable and repeatable properties, is an important drawback, because the properties of the composites can also show high standard deviations. Thus, commercial reinforcement fibers, with lower standard deviations in its mechanical properties were proposed as reinforcement. In this sense, wood pulps used for papermaking represent a worldwide available source of reinforcing fibers. Besides, such fibers were previously successfully used as polyolefin and PLA reinforcements [35,44,45].

In this paper, hybrid composite materials with two polymeric and one reinforcing phases were formulated, prepared, and tested. The two polymeric phases were both bio-based matrices, a Polylactic acid (PLA) and a thermoplastic starch-based material (PTA). The reinforcement was bleached Kraft hardwood fibers (BKHF) from the eucalyptus. The BKHF surface is mainly composed of hydroxyl groups, generating a strong hydrophilic character and hindering their adequate dispersion. However, several authors have shown that lignin could hinder the interaction between natural fibers and poly (lactic acid) [44]. This is the reason to choose this kind of fibers. Standard specimens of a blend between PTA and PLA were tested at tensile properties and compared to PP. Afterward, hybrid composites from PLA, PTA, and BKHF were also produced and tensile tested. The results were compared to BKHF reinforced PP composites. To assess the quality of the interphase a micromechanics analysis, based on a modified rule of mixtures was performed. The study has allowed us to conclude through a preliminary LCA that it is possible to obtain materials with the same properties as PP using a blend of PLA and PTA reinforced with natural fibers with a significant reduction in environmental impact.

2. Materials and methods

2.1. Materials

Polylactic acid (PLA) pellets from Nature Works (Blair, Nebraska, USA) under the trade name Ingeo biopolymer 3D870 were used as a main component of the blend. The melt flow index (MFI) and density of this PLA were 9.0 g/10 min (at 190 °C and 2.16 kg load) and 1.24 g/cc, respectively. Thermoplastic starch-based polymer (PTA) used on matrix blend preparation was a Mater-Bi YI014U/C, provided by Novamont (Novara, Italy). The MFI of this PTA was 33.36 g/10min and 1.24 g/cc of density. Bleached kraft hardwood fibers (BKHF) from eucalyptus were supplied by LECTA, S.A. (Madrid, Spain). Dichloromethane, purchased from Scharlau, S.L. (Sentmenat, Spain), was used as a solvent in the extractions for recovering the fibers from the samples. Polypropylene (PP) used as a reference polymer was Isplen PP090 62 M supplied by Repsol-YPF (Tarragona, Spain) with a MFI and density 20.0 g/10 min (at 190 °C and 2.16 kg load) and 0.905 g/cc, respectively.

2.2. Blends and composites preparation

PLA-based blends with four different PTA contents were produced: 15 wt%, 20 wt%, 25 wt%, and 30 wt%. In all cases, to prevent PLA hydrolyzation, all materials have been thoroughly dried to ensure that all moisture has been removed prior to processing. The blends with 20 wt% and 30 wt% were then compounded with different bleached kraft hardwood fibers amounts (20 and 30 wt%). The fibers were first defibrated in a Fellowmans 450 M shredder. Afterward, to remove excess moisture, the fibers and the PLA and PTA pellets were dried in an 80 °C oven for 24 h.

The PLA-PTA blends and the composites were processed in a Gelimat multikinetic mixer model G5S (Draiswerke, Mahaw, USA). The PLA-PTA blends and the fibers were introduced through the machine's feeder at 300 rpm. Then, the speed was enhanced to 2500 rpm for 2 min until discharge temperatures of 195 °C were attained. Previously, blends of

PLA-PTA without fibers were obtained by following the same method.

The obtained mixtures were pelletized in a knife mill, to keep particles having a diameter under 5 mm. The obtained granulates were injected following ISO 527–1:2000 shape specimens standard with an Aurburg 3582-D Injection machine (Lobburg, Germany). The temperature profiles range from 170 to 195 °C, and the maximum pressure during the volumetric phase was set at 50 bar while the maintenance pressure was established at 30 bar.

2.3. Blends morphological and thermal characterization

Previous to the preparation of the BKHP reinforced composite the blends from PTA and PLA were analyzed using Scanning Electron Microscope (SEM) and Differential Scanning Calorimetry (DSC). The SEM microscopy pictures were obtained with a Zeiss DSM 960A (Carl Zeiss Iberia, Madrid, Spain). All the samples required to be gold coated to ensure a correct observation. The DSC was performed to assess the influence of the PTA and the mixing of the thermal stability of PLA. A TA Instruments Q2000 (Division TA Instruments, Waters. Cerdanyola del Vallés, Spain) was used for the analysis following ASTM E 1269.01 standard. The tests were carried on in a range of 30 to 200 °C with a rate of 10 °C/min, performing two heating and controlled cooling in the same temperature range and rate. An inert atmosphere of nitrogen was used with a constant flow of 50 ml/min.

2.4. Mechanical properties

The standards ASTM D618-13 and ASTM D638-02 were followed in this research. Before mechanical testing, the samples were stabilized for 48 h in a Dycometal conditioning chamber climatic chamber at 23 °C and 50% of relative humidity. Later, at least 10 specimens were assayed to obtain the maximum strength, strain at break, and Young's modulus of the composites. Concretely, the tests were performed using a universal testing machine DTC-10 supplied by IDM test (San Sebastián, Spain), fitted with a loading cell of 5 kN and working at a speed rate of 2 mm/min. An MFA 2 extensometer, produced by MF Mess & Feienwerk technik GMBH (Velbert, Germany), was used for more precise deformation measurement. Density of composite materials was measured by means a pycnometer method according to the ISO standard ISO 1183–1.

2.5. Differential scanning calorimetry (DSC)

DSC was analyzed using a Mettler Toledo DSC822^e calorimeter (Switzerland). The samples with weight in the range of 5–10 mg were sealed in a hermetic aluminum pan and heated and cooled at 10 °C/min from 20 °C to 200 °C under nitrogen flow. two heating cycles were used, and the thermal transitions were considered for the second heating cycle to erase the thermal history. The melt crystallization temperature (Tm), Glass Transition Temperature (T_g), Crystallization temperature (T_c); Cold Crystallization Temperature (T_{cc}), and Melting temperature (T_m) were determined from the second heating scan.

The degree of crystallinity (Xc) was calculated using Equation (1):

$$\chi_c\% = \frac{(\Delta H_m - \Delta H_{cc})}{w \cdot \Delta H_m^0} \times 100 \quad (1)$$

where ΔH_m, ΔH_{cc} care the enthalpies of melting and cold crystallization, respectively. w and ΔH_m° are the weight fraction of PLA and melting enthalpy of 100% crystalline PLA, respectively. ΔH_m^0 enthalpy of meting for 100% crystalline PLA (93.6 J/g) [46].

2.6. XRD

X-ray diffraction (XRD) pattern was obtained using a Bruker D8 Advance diffractometer operating in reflection mode, with a Cu-Ka radiation, generated at 40 kV and an incident current of 30 mA. The 2 Theta angular region from 1,26° to 50° was scanned with steps of 0.02° and a step time of 3 s.

2.7. Fiber extraction for composites

Reinforcing fibers were extracted from composites by matrix solubilization, using Soxhlet apparatus and dichloromethane or decahydronaphthalene as solvents. The hybrid composite's matrices were dissolved dichloromethane whereas PP was solubilized with decahydronaphthalene. Small parts of composite specimens were pelletized and placed inside a cellulose filter and set into the Soxhlet equipment. The fiber extraction was completed after 24 h. Once the fibers were extracted, they were rinsed with acetone and water to eliminate the polymeric rests. Finally, the fibers were dried in an oven at 80 °C for 24 h.

2.8. Fiber morphology determination

Fiber's lengths distributions and diameters of the extracted BKHF were measured using a MorFi Compact (Morphological fiber analyzer), from Techpap SAS (Gières, France). An aqueous suspension of 25 mg/L of reinforcement was prepared and analyzed following the ISO/FDIS 160652 standard. The equipment measured close to 30,000 fibers. Two samples of each type of fiber were analyzed. The apparatus determines, among other, the arithmetic average (l^F), the weighted average length (l^{WF}), and diameters average (d^F) lengths.

3. Results and discussion

3.1. Mechanical and morphological characterization of the PLA/PTA blends

Before composite preparation, different PLA/PTA blends were prepared. Table 1 shows the evolution of tensile strength (σ_t^m), Young's modulus (E_t^m), and strain at break (ε_t^m) of blends at different formulations.where, V^{PTA} is the volume fraction of PTA in the blend.

The tensile strength of mono-component matrices were accounted for 50.52 MPa for PLA, and 10.56 MPa for PTA, which is significantly lower given the presence of plasticized starch that inevitably induces a notable reduction in the strength of the host matrix when blended with other polymer. In addition, Young's modulus values of PLA (3.44 GPa) revealed the high brittleness of the material in comparison with PTA, with a value of 0.17 GPa. On the other hand, PTA exhibits a much higher strain at break than PLA. These results are expected and aligned with the literature data [7,47]. In this sense, the preparation of the blends was carried out to obtain a proportional performance (see Fig. 1).

With the PTA content increasing, as expected, the tensile strength and Young's modulus of the blends decreased. The effect of PTA on the mechanical properties is more clearly observed in Fig. 2.

The rather poor quality of the interphase between PLA and thermoplastic starch-based polymers (PTA) since PLA is hydrophobic while

Table 1
Tensile characteristics of the obtained blends.

Sample	PTA (wt. %)	V^{PTA}	σ_t^m (MPa)	E_t^m (GPa)	ε_t^m (%)
PLA_{100}	0	0	50.52 ± 0.70	3.44 ± 0.08	3.42 ± 0.08
$PLA_{85}PTA_{15}$	15	0.15	40.28 ± 0.53	2.77 ± 0.06	3.40 ± 0.11
$PLA_{80}PTA_{20}$	20	0.20	37.25 ± 0.36	2.61 ± 0.07	3.24 ± 0.07
$PLA_{75}PTA_{25}$	25	0.25	34.82 ± 0.71	2.41 ± 0.04	3.18 ± 0.05
$PLA_{70}PTA_{30}$	30	0.30	31.66 ± 0.62	2.24 ± 0.09	2.99 ± 0.09
PTA_{100}	100	1	10.56 ± 0.11	0.17 ± 0.01	183.13 ± 13.09

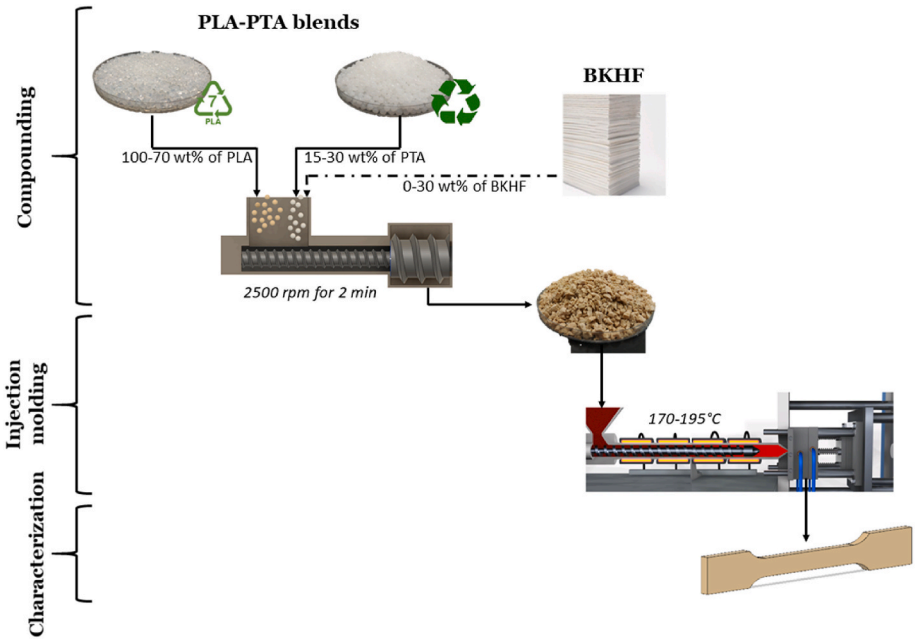

Fig. 1. Chart flow of blends and composites preparation.

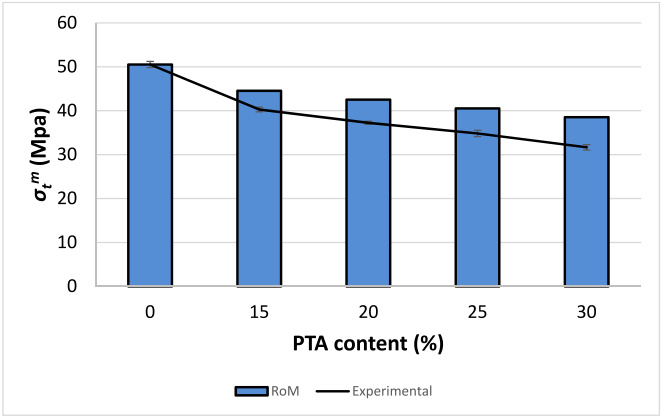

Fig. 2. Evolution of tensile strength of PLA-PTA blends.

PTA is a blend of thermoplastic starch with hydrophilic character and a biodegradable polyester such as polycaprolactone (PCL) with hydrophobic behavior has been reported [48]. As a result, this incompatibility eventually leads to inferior properties of their blends. The biggest issue with mixing both polymers rely on phase separation and non-*co*-continuity.

In this sense, the rule of mixtures (*RoM*) is a fast and simple way to detect the additive behavior of the matrices. Theoretically, the tensile strength of blends with good compatibility between the phases tends to show a linear behavior. *RoM* is expressed as:

$$\sigma_t^m = f_c \cdot \sigma_t^{PTA} \cdot V^{PTA} + \sigma_t^{PLA} \cdot \left(1 - V^{PTA}\right) \quad (2)$$

where σ_t^{PLA} and σt^{PTA} are the tensile strength of the PLA and PTA respectively, and V^{PLA} is the volumetric fraction of PLA. A linear correlation between tensile strength and PTA content was obtained, revealing a Person correlation coefficient (R^2) of 0.99. Notwithstanding, it was observed that the experimental values showed larger differences with theoretical ones as the PTA content was increased, indicating a diminution of the compatibility between the two polymers. In that sense, blends of 15%, 20%, 25% and 30% of PTA content showed compatibility yields for about 90%, 87%, 85% and 81%, respectively.

Several research groups reported in their investigations to enhance the compatibility of these two polymeric species by using a compatibilizer, by modifying the hydroxyl groups of starch, or by using coupling agents to modify starch [49,50]. The utilization of compatibilizers or coupling agents allows large-scale productions using extrusion technologies, however special and economically expensive machines are required. On the other hand, chemical modification of hydroxyl groups in starch can offer significant improvements, but sometimes it involves an expensive reactive and a large amount of harmful organic solvents [51]. Moreover, such techniques generally produce low improvements on the tensile properties compared to the costs [52].

The main advantage of PTA against PLA is its flexibility and tenacity [37]. Due to the high Young's modulus and brittleness that PLA usually exhibits, most of the PLA-based materials cannot be submitted to impact stress. Concretely, PLA presented the maximum Young's modulus at 3.44 GPa. On the other hand, Young's modulus of pure PTA was quantified in 0.17 GPa. As expected, Young's modulus of blends decreased linearly as the amount of PTA was increased. This reduction was quantified in 19%, 24%, 30%, and 35%, respectively, compared to neat PLA. As above mentioned, experimental results can be compared with the rule of mixtures for Young's modulus. In this case, the compatibility yields were in all cases close to 100%, proving the assumption that the interphase of components did not affect the stiffness of the final blend.

Concerning the strain at maximum tensile strength, PLA showed a peak poor strain of 3.42%. Due to the high strain at break of PTA (183.13%) the blends tended to gain elasticity, illustrating a second-order polynomial behavior. A high extend of strain at a maximum force of 107.38% was attained for $PLA_{20}PTA_{80}$ while the minimum value was obtained with $PLA_{70}PTA_{30}$ blend (2.99%). Nonetheless, the blend of 20% of PTA also exhibited a lower maximum strain than the pure PLA. As showed with tensile strength, blends exhibited a non-linear tendency. One possible explanation for this phenomenon could be the generation of voids between the polymers (Fig. 3). Such voids could provoke the diminution of the interfacial shear strengths between the polymers and therefore, the shrinkage of the strains.

Comparing the tensile properties of the PP, the commercial and oil-based matrix used in this research, it can be validated that PLA-PTA blends could act as a replacing product. In that sense, the tensile strength of neat PP was recorded as 27.6 MPa. From the exposed results in Table 1, it can be estimated that $PLA_{61}PTA_{39}$ blend composition

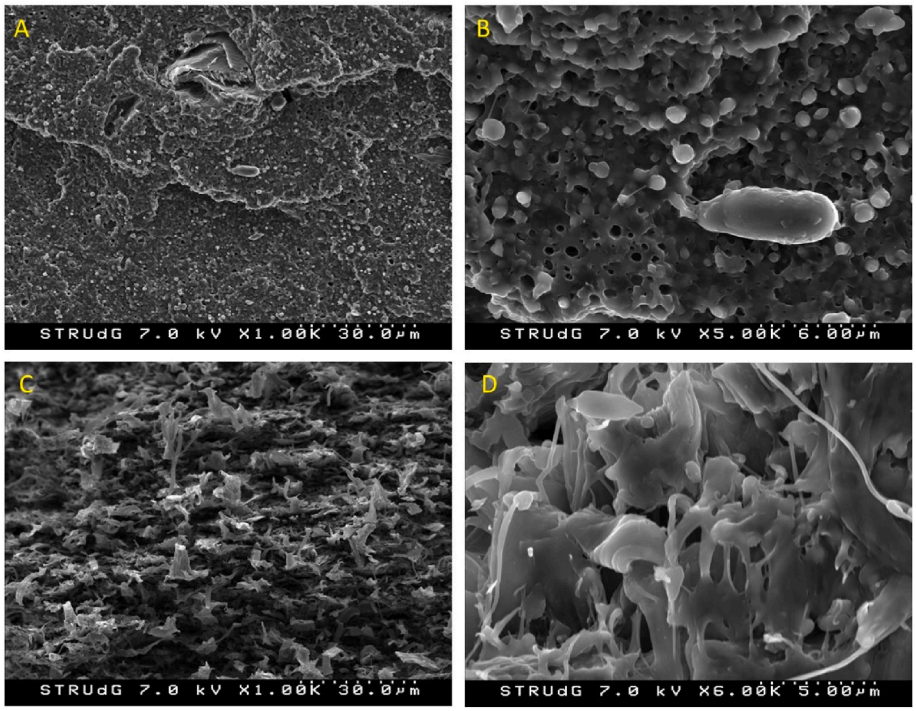

Fig. 3. SEM pictures of $PLA_{80}PTA_{20}$ (a and b) and $PLA_{70}PTA_{30}$ (c and d) at different magnifications.

would attain the same value. Likewise, Young's modulus of PP was 1.50 GPa while $PLA_{61}PTA_{39}$ was predicted for 2.05 GPa. Concerning the strain at the peak force, $PLA_{61}PTA_{39}$ will exhibit similar behaviors to the PP (14.58% versus 9.30%, respectively).

The morphology of the PLA-PTA blends was analyzed by SEM observation of the tensile fractures of the samples.

According to the content in PTA, a huge difference in the morphology of the blend can be seen (Fig. 3). At 20% PTA content ($PLA_{80}PTA_{20}$) the blend showed a typical dispersed morphology where the PTA phase is distributed in the form of spherical particles about 1–4 µm in size, within the PLA. The morphology completely changed at 30% PTA content, where the elongated fibrillar structure could be seen with both PLA and PTA phases, which is indicative of a fully continuous structure. In fact, it is known that the composition where a transition between dispersed morphology to noncontinuous structure is strongly determined by the viscosity ratio of the individual components: the higher the viscosity of the dispersed phase, the lower is the ratio for observing co-continuous structure. In our previous work concerning PBAT/TPS blends, we have shown that this ratio was observed at a composition in PBAT/TPS between 0.65/.35 to 0.7/0.3 (*Fourati, Y., Tarrés, Q., Mutjé, P., Boufi, S. 2018. PBAT/thermoplastic starch blends: Effect of compatibilizers on the rheological, mechanical and morphological properties. Carbohydrate polymers, 199, 51–57.*)

Given the co-continuous structure, we should expect a mechanical property intermediate between those of PLA and PTA However, such a tendency was not observed especially regarding strain at break. A possible reason accounting for this divergence would be a lack of effective interfacial adhesion between the PLA and PTA phases that prevents the stress transfer between the two phases. The poor interfacial adhesion could be detected in Fig. 3B, where the dispersed PTA particles appeared to be weakly bound to the continuous PLA phase, with many of the particles being detached during the breaking test. The presence of cavitation along the fibrillar structure for $PLA_{70}PTA_{30}$ is another confirmation of the poor interfacial adhesion between PLA and PTA phases. These cavitations emerge probably during the tensile testing, where the difference in the stiffness between PTA and PLA will amplify the shear stress at the interfacial area PLA/PTA, resulting in shear-yielding and crazing for the less stiff phase.

The effect of the phases dispersion and the PTA content could have a significant effect on the PLA thermal transitions. These transitions were analyzed using DSC and Fig. 4 shows the thermograph of the second heating and Table 2 shows a resume of the main transition temperatures: Glass Transition Temperature (T_g), Crystallization temperature (T_c); Cold Crystallization Temperature (T_{cc}), and Melting temperature (T_m). The crystallinity content (X) was determined using a value of 93.6 J/g as the enthalpy of a fully crystallized PLA [53] (see Table 3).

The PLA used in this work showed the characteristic T_g at 60 °C. The no crystallization behavior during the cooling process due to the poor crystallization kinetics of neat PLA, that constitutes one of the main weakness of PLA [54]. This behavior gives rise to a huge crystallization peak during the second heating cycle (Fig. 4A), referred to as the cold crystallization peak. The crystals obtained during the T_{cc} melted in a single peak at 168.8 °C. In the case of the blends, significant differences are observed. The most important is the crystallization behavior during the cooling process. In presence of PTA, the cold crystallization peak decreased in intensity while the melting peak conserved nearly the same magnitude, which is indicative of the improvement of crystallization degree of PLA induced by the presence of PTA. This could be seen from data in Table 2, where the crystalline degree of PLA substantially increases in the presence of PTA, passing from about 16% to about 35 and 25% for $PLA_{80}PTA_{20}$ and $PLA_{70}PTA_{30}$, respectively. Presumably, the presence of the PTA dispersed phase enhanced the crystallinity by acting as a nucleating site for the crystallization of PLA. Similar results were reported by Ferri et al. pointing the effective nucleating agent for PLA [55].The higher crystallinity observed at 20% PTA content, is probably due to the difference in the morphology of the PLA-PTA blends, where the granular dispersed morphology observed at 20% PTA content would be more favorable for the crystallization of PLA rather than the fibrillar morphology observed at 30% PTA content. Another evolution observed in PLA-PTA blends concerned the increase of the melting peak Tm to about 174–175 °C, while the Tm was about 168 °C for neat PLA. Referring to the literature data, The low-temperature peak is associated with melting of α′-crystals while the high-temperature melting peak is due to melting of α-crystals which has a more ordered crystal structures

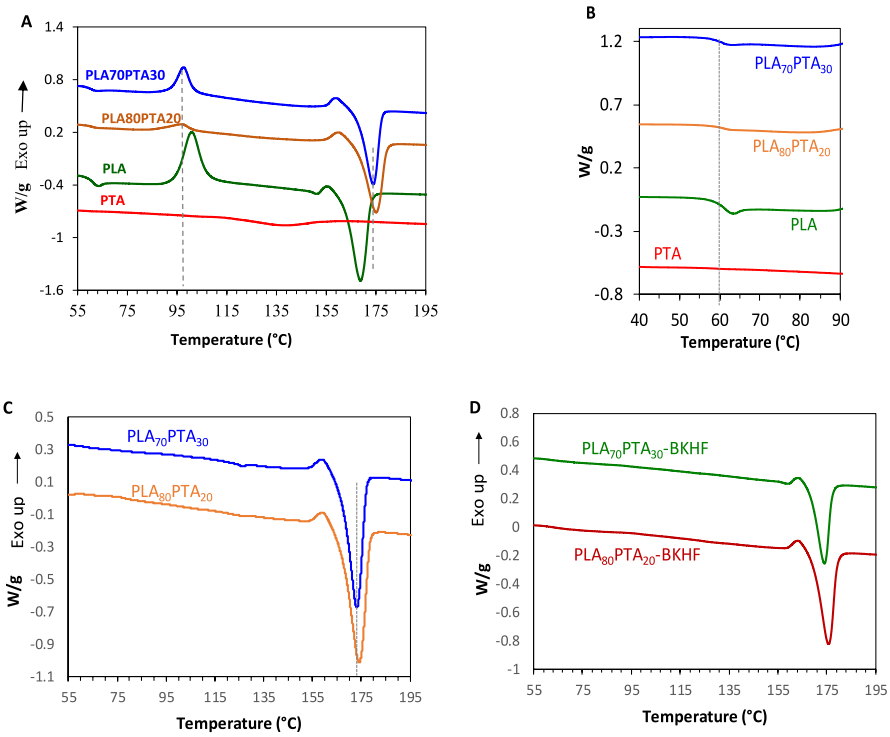

Fig. 4. (A) DSC thermogram of pure PLA, $PLA_{70}PTA_{30}$, $PLA_{80}PTA_{20}$, and PTA during the second heating, and (B) localization of the glass transition (T_g). DSC plot of (C) $PLA_{70}PTA_{30}$, $PLA_{80}PTA_{20}$ after 5 min curing at 100 °C, and (D) $PLA_{70}PTA_{30}$-BKHF, $PLA_{80}PTA_{20}$-BKHF composite at 30% fibers content.

Table 2
Thermal transition temperatures and crystallization degree of the studied materials.

Sample	T_g (°C)	T_c (°C)	T_{cc} (°C)	T_m (°C)	X_c (%)[a]	X_m (%) **
PLA_{100}	60.3	–	100.9	168.8	32.36	16.03
$PLA_{80}PTA_{20}$	60.3	97.7	96.8	175.0	4.8	35.83
$PLA_{70}PTA_{30}$	60.2	93.8	97.5	173.9	12.15	25.31
PTA_{100}	–	103.9	–	136.9	–	–
$PLA_{80}PTA_{20}$-C***	60.3	–	–	175.0	–	46
$PLA_{70}PTA_{30}$-C***	60.2	–	–	174.1	–	47
$PLA_{80}PTA_{20}$-BKHF	60.3	–	–	175	–	45
$PLA_{70}PTA_{30}$-BKHF	60.2	–	–	174	–	42

[a] Cold crystallinity degree: **Crystalline degree by subtracting the cold crystallization: *** cured samples at 100 °C during 5 min.

Table 3
Tensile strength, Strain at break and Young's modulus of the composite.

Matrix	BKHF (%)	V^F	ρ_C	σ_t^C (Mpa)	E_t^C (GPa)	ε_t^C (%)
PP	0	–	0.905	27.60 ± 0.50	1.50 ± 0.10	9.30 ± 0.30
	20	0.135	0.982	45.71 ± 0.87	3.21 ± 0.06	6.89 ± 0.22
	30	0.211	1.026	51.61 ± 0.63	4.05 ± 0.09	6.21 ± 0.17
$PLA_{70}PTA_{30}$	0	–	1.240	31.66 ± 0.42	2.24 ± 0.04	2.99 ± 0.04
	20	0.174	1.282	41.09 ± 1.21	3.87 ± 0.31	4.31 ± 0.12
	30	0.265	1.304	47.04 ± 2.78	4.75 ± 0.24	4.22 ± 0.21
	0	–	1.240	37.90 ± 1.46	2.61 ± 0.04	3.24 ± 0.07
$PLA_{80}PTA_{20}$	20	0.174	1.279	43.20 ± 0.52	4.26 ± 0.01	4.14 ± 0.06
	30	0.265	1.302	51.32 ± 0.84	5.54 ± 0.05	4.00 ± 0.26

than the α′ polymorph [56]. Accordingly, in addition to the enhancement in the crystallization of PLA by acting as nuclea, the resulting crystallite exhibites higher order.

To further support this hypothesis, XRD analysis on PLA, PTA, and PLA-PTA blends were performed on film produced by melt processing following the same procedure adopted for PLA-PTA blends (Fig. 5).

Neat PLA film is characterized by a broad halo from a $2\theta = 10°–25°$ without any diffraction peak which is indicative of an amorphous polymer (Fig. 5A) r. PTA film is characterized by multiples diffraction peaks overlying the amorphous halo indicating a semi-crystalline polymer (Fig. 5B). In PLA_xPTA_{100-x} film (x = 80 and 70), the diffraction patterns were dominated by a large halo on which weak diffraction shoulders at $2\theta = 16.8$ and 18° appeared, presumably corresponding to the crystalline part of PLA and PTA. The weak intensity of these peaks along with their broadness is suggestive of the small size of crystallites. Interestingly, it can be seen that submitting the PLA_xPTA_{100-x} blends to a short thermal treatment at 100 °C for less than 5 min induced the development of a marked crystallinity attested by the strong intense peaks at $2\theta = 16.8$ and 19.2° which are typical of the diffractions from (110)/(200) and (203) planes of PLA, respectively [57]. The same treatment conducted on PLA did not lead to the emergence of the intense crystalline peaks after the same curing time, and only after curing during 10 min at 100 °C that the typical crystalline peaks of PLA have been emerged (Fig. 5A). This confirms the aptitude of PTA dispersed phase to act as a nucleating agent promoting the crystallization of PLA. However, a post-curing treatment or an appropriate cooling cycle from the processing temperature to about 100 °C should be adopted to achieve the effective crystallization of PLA matrix.

More accurate assessment of the change in the crystalline degreeree of PLA following the short curing treatment was given from DSC analysis

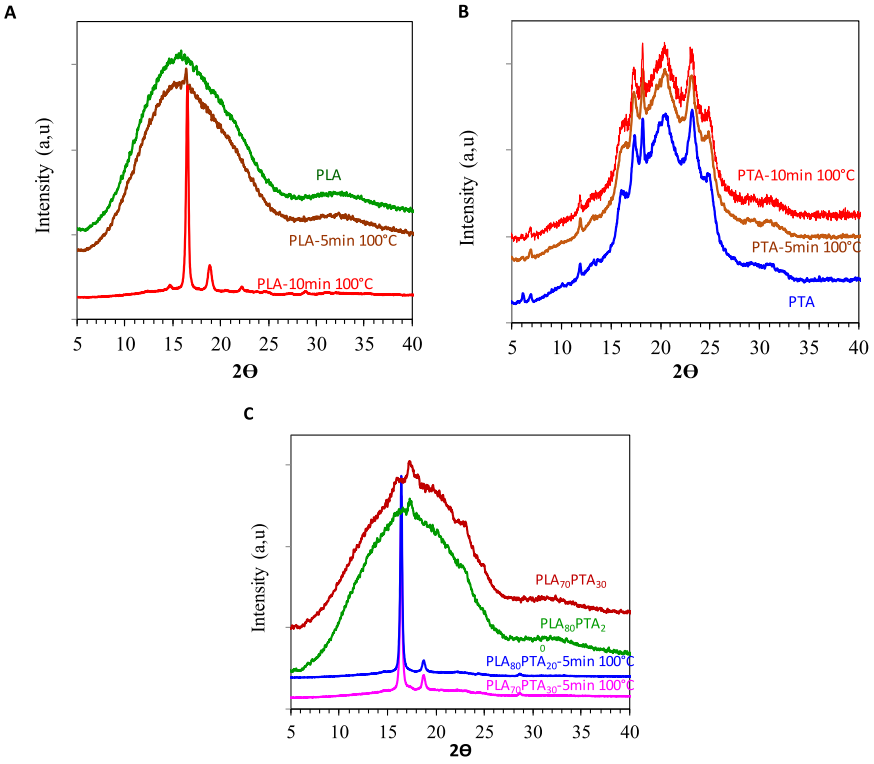

Fig. 5. XRD patterns of (A) PLA, (B) PTA, and (C) PLAxPTAy processed films before and after thermal treatment at 100 °C for 5 min (and 10 min for PLA).

(Fig. 4C), where the crystalline degree X_m attained about 47% for both cured for $PLA_{80}PTA_{20}$ and $PLA_{70}PTA_{30}$, while it was around 35 and 25% for the corresponding uncured samples. It is worth to mention that a X_m of 47% is considered as a high crystalline degree for PLA, where the maximum crystallinity for PLA was lower than 40% [58]. This demonstrates again the effectiveness of PTA present result on improving PLA crystallinity.

3.2. Tensile characteristics of composites

Experimental results of tensile strength, Young's modulus, and strain at break for the PLA_{80} PTA_{20}, $PLA_{70}PTA_{30}$, and the PP reinforced composites are shown in Table 2.

Results show that the tensile strength evolved linearly and was augmented noticeably with the increasing content of BKHF. As literature reported, the linear behavior justifies a good dispersion of the BKHF and good interphase between the fiber and the hybrid matrix [59]. Regarding the hybrid materials, there was an increase in the tensile strengths of 30% and 49%, and 30% and 52% for the reinforced with 20% w/w and 30% w/w, respectively (Fig. 6a).

Anyhow, if the values are compared with the PP-composites, these percentages were slightly lower. In that case, it was observed

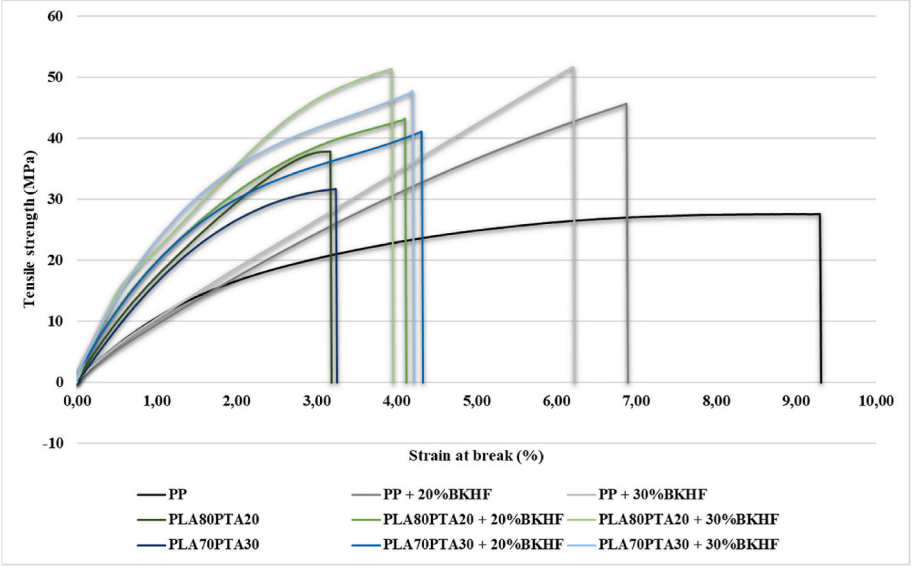

Fig. 6. Stress-strain curves for blends and composites tensile testing.

improvements of 66% and 87% in comparison with the pure PP matrix. This fact is due to the enhancement of the interphase using the MAPP coupling agent. As shown in Fig. 7, the interface between the bleached eucalyptus kraft fibers and the polypropylene matrix (Fig. 7a,b), shows a high level of bonding due to the presence of the coupling agent. The MAPP coupling agent allows the generation of ester and hydrogen bonds between the maleic anhydride groups of the coupling agent and the hydroxyl groups of the fibers. On the other hand, the coupling agent of the polymeric chain identical to the matrix is physically bound to the matrix [60–63]. For the hybrid PLA/PTA matrix composites, the absence of a coupling agent, in contrast, results in weak interfacial adhesion areas.

Nonetheless, the absolute tensile strength of hybrid composites was in line with the PP composites. Hence, from a point of view of tensile strength, BKHF reinforced hybrid composites could substitute the BKHF reinforced PP composites.

A linear increase of Young's modulus against the percentage content was observed for all tested composites, thus indicating a good dispersion of the reinforcement. Literature exposes that the interphase between the fibers and the matrix has little influence on Young's modulus of a composite [64]. Nonetheless, the increases in Young's modulus varied with the matrices. In this sense, Young's modulus of $PLA_{70}PTA_{30}$ and $PLA_{80}PTA_{20}$ composites with 20% and 30% BKHF were 71% and 112%, and 63% and 112% higher than hybrid matrix, respectively. On the other hand, the PP-composites reinforced with 20% w/w and 30% w/w showed increases of its Young's modulus of 114% and 170%. Nonetheless, hybrid-composites still exhibited higher Young's modulus than BKHF reinforced PP-composites at the same reinforcement percentage. This is because Young's modulus of PP was 49% and 74% lesser than $PLA_{70}PTA_{30}$ $PLA_{80}PTA_{20}$ pure hybrids. Thus, from a perspective of stiffness, it is presumed that hybrid composites can replace the PP composites.

Compared to neat matrices, the studied hybrid composites revealed noticeable increments of strain at maximum stress. BKHF reinforced hybrid composites presented improvements between 25 and 45%. Unlike hybrid composites, the strain at maximum force of the PP composites decreased significantly when the percentage of reinforcement was increased.

It is widely known that the strengthening ability of the reinforcement can be affected by the intrinsic properties of the fiber, the typology of bonds between fiber and matrix, and the number of bonds per volume unit. Anyway, the interphase between the hybrid and the fibers is not tuned. Fibers with high contents of cellulose, as in the case of BKHF, are characterized by its great mechanical properties, however present a markedly hydrophilic behavior. The elevated chemical surface gradient diminishes the interaction between the phases. Some authors revealed

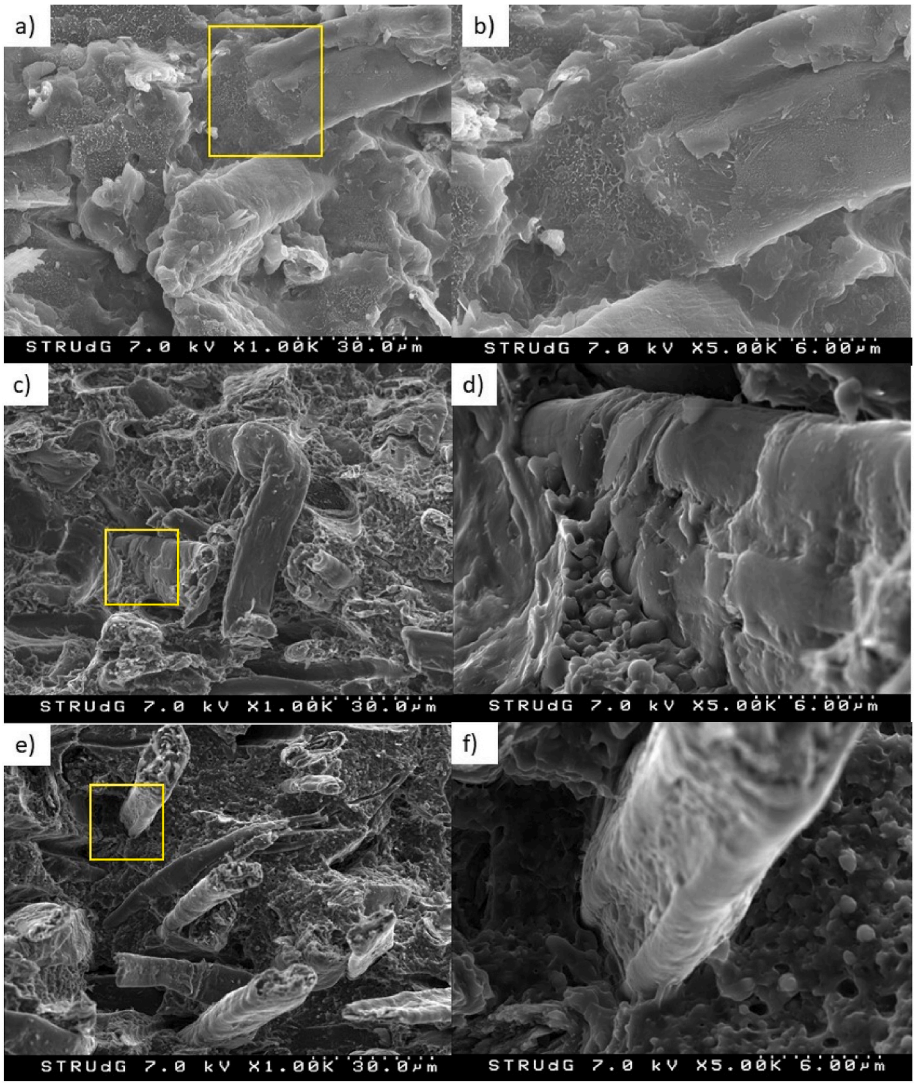

Fig. 7. SEM micrographs of 30% w/w composites: (a,b) PP with BKHF and coupling agent composite; (c,d) $PLA_{70}PTA_{30}$ with BKHF composite; (e,f) $PLA_{80}PTA_{20}$ with BKHF composite.

that fibers with lignin content might improve the dispersion of the fibers but on the other hand, its reinforcements could cause the diminution of the final tensile properties of the composites. Other authors used chemical products like diethylene glycol dimethyl ether (Diglyme) which act as dispersing agents [44].

The effect of the inclusion of BKHF cellulose fibers on the crystalline degree of PLA in PLA-PTA composites was assessed at 30% fibers loading (Fig. 4D). Xm was around 45% and 42% for $PLA_{70}PTA_{30}$ and $PLA_{80}PTA_{20}$ composites, respectively. this level was higher than that observed in the blend without fibers (around 25–35%), meaning that the presence of BKHF cellulose fibers further enhanced the crystallization of PLA phase, presumably by acting as a nucleating agent. The increment in the crystalline degree of PLA in PLA-PTA-BKHF composites would also beneficially contribute to the enhancement in the modulus of the composite as the crystalline phase would act as reinforcement. By preventing the cold crystallization to occur, the presence of BKHF fibers would expend the operating temperature over 100 °C, which contributes to alleviate one of the shortcomings of PLA.

It is worth to mention that the mechanical properties of PLA-PTA-BKHF composites did not undergone any meaningful evolution in terms of tensile modulus or strength after storing for more than 3 months at 23 °C and 50% RH. It is likely that the presence of the cellulose fibers within the heterogenous PLA/PTA blends contributed to maintain the mechanical properties of the composites. Given the key role of cellulose fibers in the reinforcement of the composites, we presume that the inclusion of the fibers at 30% loading contributed to stabilize the mechanical properties of the material.

4. Micromechanics

Focusing on the tensile properties of the semi-aligned reinforced composites, multiple predictions have been presented to model the tensile properties of reinforced composites. One of the easiest but consistent models is a modified rule of mixtures (mRoM) for the tensile strength and Young's modulus [65]:

$$\sigma_t^C = \chi_1 \cdot \chi_2 \cdot \sigma_t^F \cdot V^F + \left(1 - V^F\right) \cdot \sigma_t^{m*} \tag{3}$$

$$E_t^C = \eta_l \cdot \eta_o \cdot E_t^F \cdot V^F + \left(1 - V^F\right) \cdot E_t^m \tag{4}$$

As shown in Equation (2), σ_t^C is the ultimate tensile strength of the composite, σ_t^F is the intrinsic tensile strength of the reinforcement, χ_1 and χ_2 are the orientation and the length factors, used to modulate the contribution of the semi-aligned short fiber reinforcement, V^F is the volume fraction of reinforcement and σ_t^{m*} is the contribution of the matrix at the ultimate strain of the composite. The coupling factor is described as the product of the orientation and length factor ($f_c = \chi_1 \cdot \chi_2$). In the case of semi-aligned composites, it is reported in the literature that good fiber-matrix interphases show coupling factors between 0.18 and 0.2 [66].

On the other hand, E_t^C, E_t^M, and E_t^F are Young's modulus of the composite, the matrix, and the reinforcement, respectively. η_l and η_o are the modulus length and orientation efficiency factors, respectively, used to equalize the contribution of the semi-aligned short reinforcement fibers. The efficiency factor is computed as the multiplication of the length factor and orientation factor ($\eta_e = \eta_l \cdot \eta_o$). According to the literature, the efficiency factor can be expected in a range from 0.4 to 0.6 [67].

Nonetheless, with the experimental data at hand, such an equation is undetermined. The mRoM necessarily requires the intrinsic tensile strength and Young's modulus of the reinforcement. However, due to their length, the measure of such parameters is almost impossible. In addition, there is a discrepancy in the use of experimental values to model the tensile behavior of a composite. Therefore, the application of alternative methods is required to determine the intrinsic properties of the fibers. In previous work, the authors proposed a fiber tensile strength factor (FTSF) and fiber tensile modulus factor (FTMF) [68]. The FTSF and FTMF define the strengthening and stiffening capacity of the reinforcing fibers to the final strength of the composite. The calculus of FTSF and FTMF are achieved by rearranging the RoM:

$$FTSF = \frac{\sigma_t^C - \left(1 - V^F\right) \cdot \sigma_t^{m*}}{V^F} = \chi_1 \cdot \chi_2 \cdot \sigma_t^F \tag{5}$$

$$FTMF = \frac{E_t^C - \left(1 - V^F\right) \cdot E_t^m}{V^F} = \eta_l \cdot \eta_o \cdot E_t^F \tag{6}$$

where the term $\sigma_t^C \cdot f_c$is related to the fiber contribution to the composite tensile strength, and the FTSF represents the slope of the regression curve. FTSF were presented in Fig. 8.

The *FTSF* of the BKHF reinforced $PLA_{70}PTA_{30}$ and $PLA_{80}PTA_{20}$ composites rendered values of 88.69 and 88.54 MPa, respectively. The variations of the pure matrices content did not produce a significant variation of the FTSF. Nonetheless, such values were lower than PP reinforced with the same amount of fiber (147.34), demonstrating therefore that BKHF performs better interfacial bonding with PP.

Unlike FTSF, the BKHF reinforced hybrid composites showed a FTMF of 11.68 and 13.54 while PP composites delivered a value of 13.75. The close FTMF values for the BKHF composites might denote a similar stiffening capability despite the matrix. As above commented, Young's modulus is barely affected by the quality of the interfacial adhesion.

To study the intrinsic tensile strength of the fibers and the quality of the interphase, a micromechanical analysis was carried out. Equation (2) presents two unknowns, the coupling factor ($f_c = \chi_1 \cdot \chi_2$) and the intrinsic tensile strength of the reinforcement. Nonetheless, as above mentioned, the literature shows that the coupling factor usually remains in the range from 0.18 to 0.2 for composites with strong interphases. Thus, to compute a theoretical value for the intrinsic tensile strength of

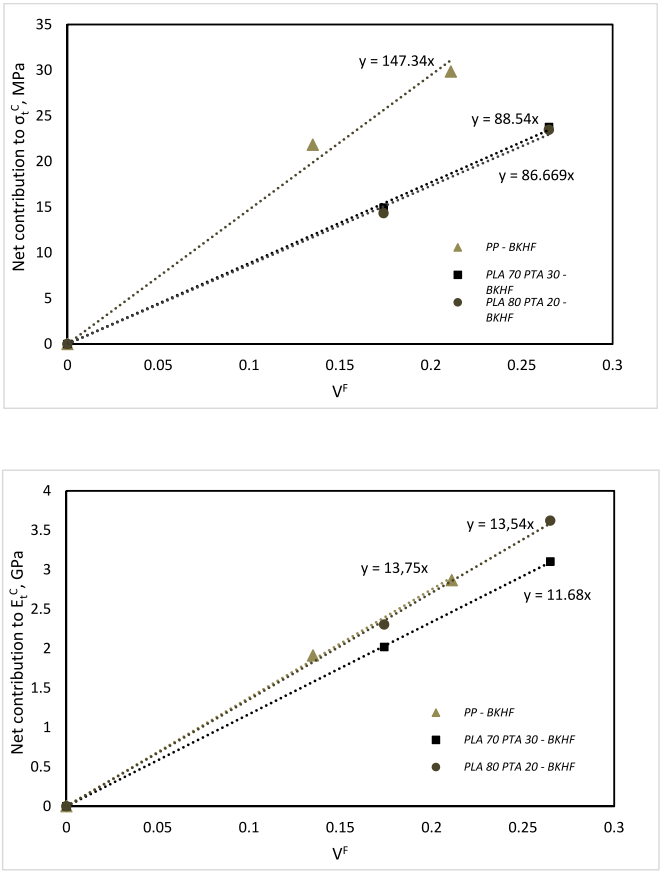

Fig. 8. Net Contributions of the reinforcement to the tensile strength and Young's modulus of the composite.

BKHF as PLA/PTA reinforcement, the value of the coupling factor was assumed to be in the range from 0.18 to 0.2. If such values are used with equation (2), the intrinsic tensile strength of BKHF is in the range of 341–498 MPa. The results obtained are slightly higher than those evaluated experimentally for other natural fibers such as jute fibers (258–314 MPa) [69].Although it is in the same range (300–600 MPa) as other natural fibers of non-wood origin [70], the values obtained are lower than those reported in the literature for wood fibers (1000 MPa) [71].This significant difference in the intrinsic resistance calculated for BKHFs may be largely caused by a lower interface than that obtained in compounds with PP, as mentioned previously. In this sense, an intrinsic tensile strength value of 1000 MPa in Equation (2) would lead to a coupling factor (f_c) of 0.1.

As previously mentioned, the RoM for Young's modulus of a composite (Equation (3)) presents irresoluble unknowns through experimental methods. Alternatively, several authors propose the use of micromechanical models to evaluate the intrinsic tensile properties of the fibers. In that sense, Hirsch's model was a widely used method to calculate the fiber's intrinsic Young's modulus from the experimental data [72].

$$E_t^C = \beta \cdot \left(E_t^F \cdot V^F + E_t^m \cdot \left(1 - V^F\right)\right) + (1-\beta)\frac{E_t^F \cdot E_t^m}{E_t^m \cdot V^F + E_t^F \cdot \left(1 - V^F\right)} \quad (7)$$

where E_t^C, E_t^F, E_t^m are the elastic modulus of the composite, the reinforcement, and the matrix respectively, V^F is the reinforcement volume fraction and the factor β is related to the stress transfer between the fiber and the matrix. In previous works, a value of $\beta = 0.4$ reproduced accurately the experimental data for semi-aligned short-fiber reinforced composites [67].Using the experimental data in equation (6), a range of values of intrinsic elastic modulus of the bleached kraft hardwood fibers between 21.96 and 25.64 GPa has been obtained for the different compounds. In contrast to the tensile strength, the intrinsic modulus obtained from the modeling is similar to the literature values for commercial bleached eucalyptus kraft pulp (30 MPa) [73]. This is due to the fact that the interface does not have important relevance in the young's modulus of the composites. Nevertheless, it is determinant for the achievement of important tensile strength increment values.

4.1. Preliminary LCA

The sustainability of a material is usually assumed as a function of its origin. However, only by using a life cycle analysis different materials can be compared and ensure that the chosen alternative is more sustainable than the substituted material. However, conducting full life cycle analysis studies requires a large amount of information that is not always available. For this reason, conducting preliminary life cycle analyses using literature data and studying the main impact factors can be used as a clear indication of the sustainability of the proposed alternatives [74,75]. A preliminary LCA was carried out by using the sustainability package of the Solid Works program and bibliographic data of the different materials studied [16,76–78]. The impact factors studied were the carbon footprint, water eutrophication, air acidification, and total energy consumed. For this preliminary analysis, the production and use of these materials have been assumed in Europe with a life span of 10 years. At the end of this useful life, it has been considered that the materials with fiberglass are incinerated, while the others are 60% recycled, 30% are incinerated and the remaining 10% end up in landfills.

Initially, the four environmental impacts mentioned above have been studied for the different PLA PTA blends proposed and compared with the impacts of the three polymeric matrices studied.

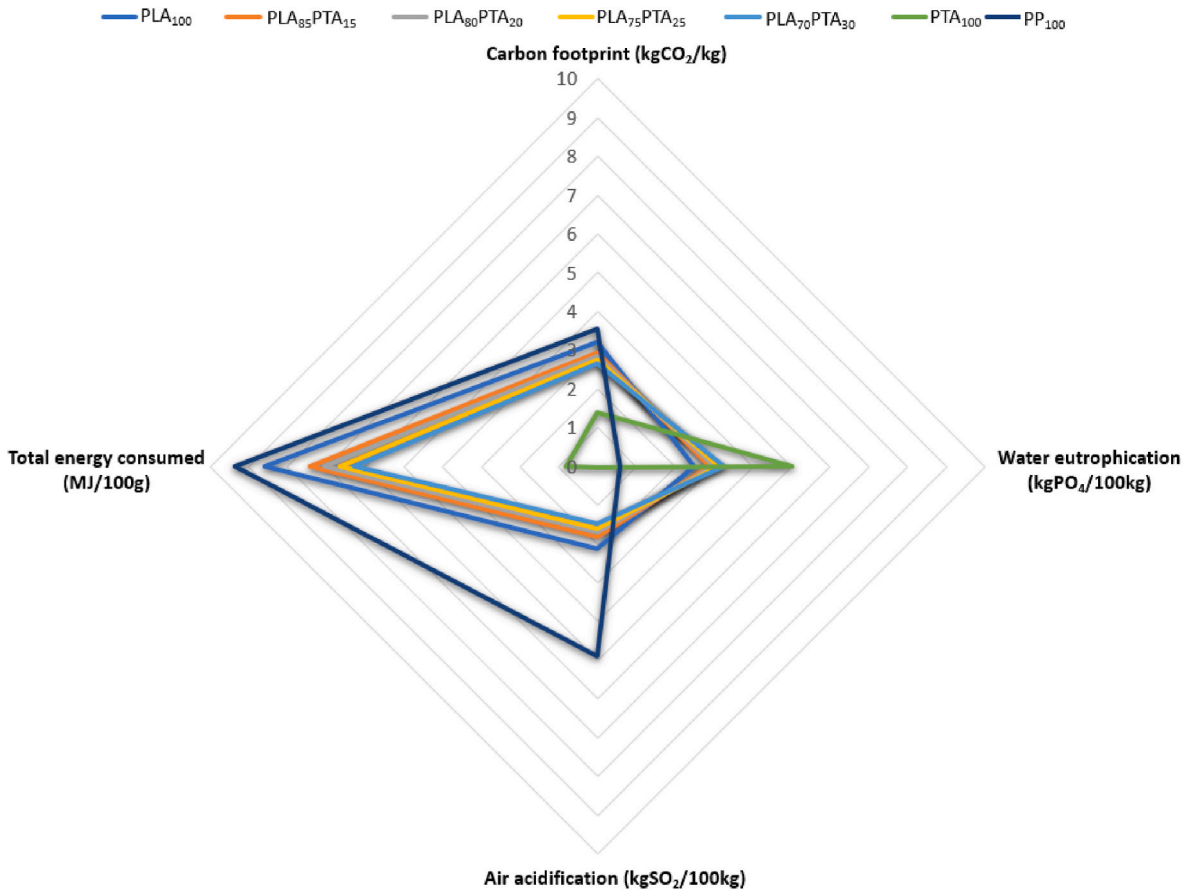

Fig. 9. Preliminary LCA of pure polymeric matrices and the obtained blends.

The results presented in Fig. 9 show the PTA matrix with the lowest values for the impacts of carbon footprint, air acidification, and total energy consumed. On the contrary, the presence of a high starch content causes a higher impact in terms of water eutrophication. The PLA matrix has an impact value in water eutrophication lower than PTA, which leads to blends with lower impacts of carbon footprint, total energy consumed, and air acidification than PLA and lower impact of water eutrophication than PTA.

Blends used for the preparation of the composite materials, $PLA_{80}PTA_{20}$ and $PLA_{70}PTA_{30}$, obtained a reduction in the carbon footprint of 24.8 and 33.2%, air acidification of 188 and 228%, and total energy consumed of 33 and 49% compared to polypropylene, respectively. However, for the water eutrophication indicator, this impact is higher by 412% and 555% compared to polypropylene.

Finally, the evolution of these indicators was studied for the composites obtained and compared with the composites with polypropylene and glass fiber (Fig. 10).

The results obtained confirm the greater sustainability of composite materials with bleached eucalyptus kraft fibers compared to blends. Likewise, these composites again show a lower environmental impact in three of the four indicators analyzed. Again, although with a minor difference, the composites obtained have a higher impact on water eutrophication. For the correct comparison of the different materials, the different density of the materials has been taken into account. Knowing that the same piece will have a lower weight in the case of using PP as matrix or a lower content of reinforcement fiber. In the case of applications of these materials such as the automotive sector where weight is key to reducing fuel consumption, a deeper environmental analysis should be carried out. This preliminary analysis of LCA shows that the incorporation of a higher content of natural fibers reduces the environmental impact of the obtained material.

5. Conclusions

Aiming to substitute PP and PP-based wood composites, blend of PLA with PTA and their composite form by adding BKHF were prepared by melt processing. The objective was to tune the mechanical performance of the material by an appropriate based on PLA, PTA, and BKHF so that compostable material competitive with PP/BKHF composites in terms of stiffness and strength could be produced. In the first part of the work, it was shown that the inclusion of PTA in PLA negatively affected both the tensile strength and Young's modulus of the blends, while holding the brittleness of PLA. The incorporation of PTA into a PLA matrix was intended to increase the compostability of the material. This addition caused the tensile strength to decrease by 37.3%, Young's modulus to decrease by 34.9% and the deformation to decrease by 12.6% for the blend with 30% PTA. However, the addition of bleached kraft hardwood fibers (BKHF) improved its mechanical performance. In the case of the blend with 20% PTA reinforced with 30% BKHF, a tensile strength of 51.32 MPa (35.4% increase), a Young's modulus of 5.54 GPa (112.3% increase) and a strain of 4% (23.5% gain) were obtained. A linear increase of Young's modulus against the percentage content was observed for all tested composites indicating effective dispersion of the reinforcement. Micromechanical models were used to fit the mechanical behavior of the composite and further predict the mechanical properties according to the fibers content. Beyond their reinforcing effect, the presence of BKHF fibers enhanced the crystallinity of PLA to a high level exceeding 40%, thanks to their nucleating effect. This prevents the cold crystallization to took place which would be beneficial for application where thermal stability over 50 °C is needed. LCA was carried out by using the sustainability package of the Solid Works program and bibliographic data of the different materials studied. The impact factors studied were the carbon footprint, water eutrophication, air

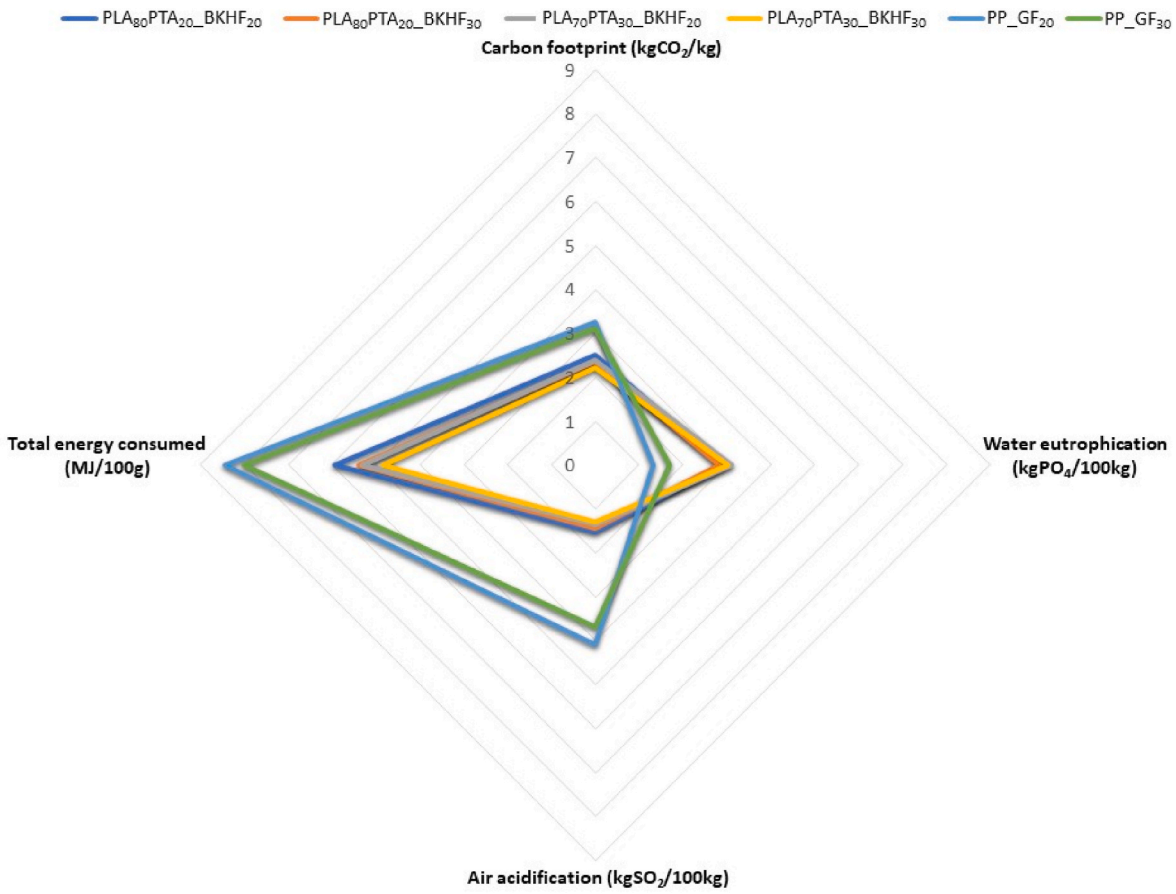

Fig. 10. Preliminary LCA of PLA/PTA blends composites and polypropylene composites.

acidification, and total energy consumed. It was shown that PTA matrix with the lowest values for the impacts of carbon footprint, air acidification, and total energy consumed. On the contrary, the presence of a high starch content causes a higher impact in terms of water eutrophication. The PLA matrix has an impact value in water eutrophication lower than PTA, which leads to blends with lower impacts of carbon footprint, total energy consumed, and air acidification than PLA and lower impact of water eutrophication than PTA. The highest sustainability was achieved with the PLA/PTA/BKHF composites, with the lowest environmental impact. This preliminary analysis of LCA shows that the incorporation of a higher content of natural fibers reduces the environmental impact of the obtained material. The study has also allowed to conclude through a preliminary LCA that it is possible to obtain materials with the same properties of PP with a 33.6% reduction of the carbon footprint. Work is under progress to reduce the brittleness of the composite by the inclusion of a reactive coupling agent based on maleated polyester.

Funding

This research was funded by the MAT2017-83347-R grant of the Spanish Ministry of Economy and Competitiveness.

CRediT authorship contribution statement

Ferran Serra-Parareda: Investigation, Methodology. **Marc Delgado-Aguilar:** Investigation, Data curation, Writing – original draft. **Francesc X. Espinach:** Investigation, Methodology, Formal analysis, writing-review. **Pere Mutjé:** Supervision, Resources, Project administration, writing-review. **Sami Boufi:** Supervision, Resources, Project administration, writing-review. **Quim Tarrés:** Supervision, Validation, Writing – original draft, Writing – review & editing.

Declaration of competing interest

The authors declare that they have no known competing financial interests or personal relationships that could have appeared to influence the work reported in this paper.

Acknowledgment

The authors wish to acknowledge the University of Girona and the University of Sfax for providing the basic resources to develop this research. Dr. Marc Delgado-Aguilar is a Serra Húnter Fellow.

References

[1] Allen S, Allen D, Phoenix VR, Le Roux G, Durántez Jiménez P, Simonneau A, et al. Atmospheric transport and deposition of microplastics in a remote mountain catchment. Nat Geosci 2019;12:339–44.
[2] Wang J, Yuan X, Deng S, Zeng X, Yu Z, Li S, et al. Waste polyethylene terephthalate (PET) plastics-derived activated carbon for CO2capture: a route to a closed carbon loop. Green Chem 2020;22:6836–45. https://doi.org/10.1039/d0gc01613f.
[3] Cox KD, Covernton GA, Davies HL, Dower JF, Juanes F, Dudas SE. Human consumption of microplastics. Environ Sci Technol 2019;53:7068–74. https://doi.org/10.1021/acs.est.9b01517.
[4] Vinod A, Sanjay MR, Suchart S, Jyotishkumar P. Renewable and sustainable biobased materials: an assessment on biofibers, biofilms, biopolymers and biocomposites. J Clean Prod 2020;258. https://doi.org/10.1016/j.jclepro.2020.120978.
[5] Jiang X, Yu Y, Guan Y, Liu T, Pang C, Ma J, et al. Random and multiblock PBS copolyesters based on a rigid diol derived from naturally occurring camphor: influence of chemical microstructure on thermal and mechanical properties. ACS Sustainable Chem Eng 2020;8:3626–36. https://doi.org/10.1021/acssuschemeng.9b06326.
[6] Meereboer KW, Misra M, Mohanty AK. Review of recent advances in the biodegradability of polyhydroxyalkanoate (PHA) bioplastics and their composites. Green Chem 2020;22:5519–58. https://doi.org/10.1039/d0gc01647k.
[7] Ge C, Lansing B, Lewis CL. Thermoplastic starch and poly(vinyl alcohol) blends centered barrier film for food packaging applications. Food Packag Shelf Life 2021;27. https://doi.org/10.1016/j.fpsl.2020.100610.
[8] Xu A, Wang Y, Gao J, Wang J. Facile fabrication of a homogeneous cellulose/polylactic acid composite film with improved biocompatibility, biodegradability and mechanical properties. Green Chem 2019;21:4449–56. https://doi.org/10.1039/c9gc01918a.
[9] Muthuraj R, Misra M, Mohanty AK. Injection molded sustainable biocomposites from poly(butylene succinate) bioplastic and perennial grass. ACS Sustainable Chem Eng 2015;3:2767–76. https://doi.org/10.1021/acssuschemeng.5b00646.
[10] Smith MKM, Paleri DM, Abdelwahab M, Mielewski DF, Misra M, Mohanty AK. Sustainable composites from poly(3-hydroxybutyrate) (PHB) bioplastic and agave natural fibre. Green Chem 2020;22:3906–16. https://doi.org/10.1039/d0gc00365d.
[11] Mittal G, Rhee KY, Mišković-Stanković V, Hui D. Reinforcements in multi-scale polymer composites: processing, properties, and applications. Compos B Eng 2018;138:122–39. https://doi.org/10.1016/j.compositesb.2017.11.028.
[12] Vieira PR, Carvalho EML, Vieira JD, Toledo Filho RD. Experimental fatigue behavior of pultruded glass fibre reinforced polymer composite materials. Compos B Eng 2018;146:69–75. https://doi.org/10.1016/j.compositesb.2018.03.040.
[13] Fliegener S, Kennerknecht T, Kabel M. Investigations into the damage mechanisms of glass fiber reinforced polypropylene based on micro specimens and precise models of their microstructure. Compos B Eng 2017;112:327–43. https://doi.org/10.1016/j.compositesb.2016.12.051.
[14] Lekube BM, Hermann W, Burgstaller C. Partially compacted polypropylene glass fiber non-woven composite: influence of processing, porosity and fiber length on mechanical properties and modeling. Compos Part A Appl Sci Manuf 2020:135. https://doi.org/10.1016/j.compositesa.2020.105939.
[15] Wang BJ, Lee JY, Wang RC. Fiberglass dermatitis: report of two cases. J Formos Med Assoc 1993;92:755–8.
[16] Joshi SV, Drzal LT, Mohanty AK, Arora S. Are natural fiber composites environmentally superior to glass fiber reinforced composites? Compos Part a-Applied Sci Manuf 2004;35:371–6. https://doi.org/10.1016/j.compositesa.2003.09.016.
[17] Martinez Villadiego K, Arias Tapia MJ, Useche J, Escobar Macías D. Thermoplastic starch (TPS)/Polylactic acid (PLA) blending methodologies: a review. J Polym Environ 2021. https://doi.org/10.1007/s10924-021-02207-1.
[18] Yan L, Kasal B, Huang L. A review of recent research on the use of cellulosic fibres, their fibre fabric reinforced cementitious, geo-polymer and polymer composites in civil engineering. Compos B Eng 2016;92:94–132. https://doi.org/10.1016/J.COMPOSITESB.2016.02.002.
[19] Pickering KL, Efendy MGA, Le TM. A review of recent developments in natural fibre composites and their mechanical performance. Compos Part A Appl Sci Manuf 2016;83:98–112.
[20] Gholampour A, Ozbakkaloglu T. A review of natural fiber composites: properties, modification and processing techniques. characterization, applications, vol. 55. Springer US; 2020. https://doi.org/10.1007/s10853-019-03990-y.
[21] La Rosa AD, Recca G, Summerscales J, Latteri A, Cozzo G, Cicala G. Bio-based versus traditional polymer composites. A life cycle assessment perspective. J Clean Prod 2014;74:135–44. https://doi.org/10.1016/j.jclepro.2014.03.017.
[22] Beckermann GW, Pickering KL. Engineering and evaluation of hemp fibre reinforced polypropylene composites: micro-mechanics and strength prediction modelling. Compos Part A Appl Sci Manuf 2009;40:210–7. https://doi.org/10.1016/j.compositesa.2008.11.005.
[23] Tarrés Q, Vilaseca F, Herrera-Franco PJ, Espinach FX, Delgado-Aguilar M, Mutjé P. Interface and micromechanical characterization of tensile strength of bio-based composites from polypropylene and henequen strands. Ind Crop Prod 2019;132:319–26. https://doi.org/10.1016/j.indcrop.2019.02.010.
[24] Mohanty S, Verma SK, Nayak SK. Dynamic mechanical and thermal properties of MAPE treated jute/HDPE composites. Compos Sci Technol 2006;66:538–47. https://doi.org/10.1016/j.compscitech.2005.06.014.
[25] Robertson NLM, Nychka JA, Alemaskin K, Wolodko JD. Mechanical performance and moisture absorption of various natural fiber reinforced thermoplastic composites. J Appl Polym Sci 2013;130:969–80. https://doi.org/10.1002/app.39237.
[26] Anastas P, Warner J. Green chemistry: theory and practice. Oxford Oxford Univ Press; 1998.
[27] da Silva D, Kaduri M, Poley M, Adir O, Krinsky N, Shainsky-Roitman J, et al. Biocompatibility, biodegradation and excretion of polylactic acid (PLA) in medical implants and theranostic systems. Chem Eng J 2018;340:9–14. https://doi.org/10.1016/j.cej.2018.01.010.
[28] Nofar M, Salehiyan R, Ciftci U, Jalali A, Durmuş A. Ductility improvements of PLA-based binary and ternary blends with controlled morphology using PBAT, PBSA, and nanoclay. Compos B Eng 2020:182. https://doi.org/10.1016/j.compositesb.2019.107661.
[29] Hamad K, Kaseem M, Ayyoob M, Joo J, Deri F. Polylactic acid blends: the future of green, light and tough. Prog Polym Sci 2018;85:83–127. https://doi.org/10.1016/j.progpolymsci.2018.07.001.
[30] Akindoyo JO, Beg MDH, Ghazali S, Heim HP, Feldmann M. Impact modified PLA-hydroxyapatite composites – thermo-mechanical properties. Compos Part A Appl Sci Manuf 2018;107:326–33. https://doi.org/10.1016/j.compositesa.2018.01.017.
[31] Flores-Hernández CG, Colín-Cruz A, Velasco-Santos C, Castaño VM, Rivera-Armenta JL, Almendarez-Camarillo A, et al. All green composites from fully renewable biopolymers: chitosan-Starch reinforced with Keratin from feathers. Polymers 2014;6:686–705. https://doi.org/10.3390/polym6030686.
[32] Fazeli M, Florez JP, Simão RA. Improvement in adhesion of cellulose fibers to the thermoplastic starch matrix by plasma treatment modification. Compos B Eng 2019;163:207–16. https://doi.org/10.1016/j.compositesb.2018.11.048.

[33] Fourati Y, Tarrés Q, Mutjé P, Boufi S. PBAT/thermoplastic starch blends: effect of compatibilizers on the rheological, mechanical and morphological properties. Carbohydr Polym 2018;199. https://doi.org/10.1016/j.carbpol.2018.07.008.
[34] Saini P, Arora M, Kumar MNVR. Poly(lactic acid) blends in biomedical applications. Adv Drug Deliv Rev 2016;107:47–59. https://doi.org/10.1016/j.addr.2016.06.014.
[35] Delgado-Aguilar M, Julián F, Tarrés Q, Méndez JA, Mutjé P, Espinach FX. Bio composite from bleached pine fibers reinforced polylactic acid as a replacement of glass fiber reinforced polypropylene, macro and micro-mechanics of the Young's modulus. Compos B Eng 2017;125. https://doi.org/10.1016/j.compositesb.2017.05.058.
[36] Zhao X, Li K, Wang Y, Tekinalp H, Larsen G, Rasmussen D, et al. High-strength polylactic acid (PLA) biocomposites reinforced by epoxy-modified pine fibers. ACS Sustainable Chem Eng 2020;8:13236–47. https://doi.org/10.1021/acssuschemeng.0c03463.
[37] Jiménez AM, Espinach FX, Delgado-Aguilar M, Reixach R, Quintana G, Fullana-i-Palmer P, et al. Starch-based biopolymer reinforced with high yield fibers from sugarcane bagasse as a technical and environmentally friendly alternative to high density polyethylene. Bioresources 2016;11:9856–68. https://doi.org/10.15376/biores.11.4.9856-9868.
[38] Yusoff RB, Takagi H, Nakagaito AN. Tensile and flexural properties of polylactic acid-based hybrid green composites reinforced by kenaf, bamboo and coir fibers. Ind Crop Prod 2016;94:562–73. https://doi.org/10.1016/j.indcrop.2016.09.017.
[39] Bledzki AK, Franciszczak P, Meljon A. High performance hybrid PP and PLA biocomposites reinforced with short man-made cellulose fibres and softwood flour. Compos Part A Appl Sci Manuf 2015;74:132–9. https://doi.org/10.1016/j.compositesa.2015.03.029.
[40] Ashori A. Hybrid composites from waste materials. J Polym Environ 2010;18:65–70. https://doi.org/10.1007/s10924-009-0155-6.
[41] Nofar M, Sacligil D, Carreau PJ, Kamal MR, Heuzey MC. Poly (lactic acid) blends: processing, properties and applications. Int J Biol Macromol 2019;125:307–60. https://doi.org/10.1016/j.ijbiomac.2018.12.002.
[42] Dicker MPM, Duckworth PF, Baker AB, Francois G, Hazzard MK, Weaver PM. Green composites: a review of material attributes and complementary applications. Compos Part A Appl Sci Manuf 2014;56:280–9. https://doi.org/10.1016/j.compositesa.2013.10.014.
[43] Reixach R, Espinach FX, Arbat G, Julián F, Delgado-Aguilar M, Puig J, et al. Tensile properties of polypropylene composites reinforced with mechanical, thermomechanical, and chemi-thermomechanical pulps from orange pruning. Bioresources 2015;10:4544–56. https://doi.org/10.15376/biores.10.3.4544-4556.
[44] Granda LA, Espinach FX, Tarrés Q, Méndez JA, Delgado-Aguilar M, Mutjé P. Towards a good interphase between bleached kraft softwood fibers and poly(lactic) acid. Compos B Eng 2016;99. https://doi.org/10.1016/j.compositesb.2016.05.008.
[45] Agnantopoulou E, Tserki V, Marras S, Philippou J, Panayiotou C. Development of biodegradable composites based on wood waste flour and thermoplastic starch. J Appl Polym Sci 2010;126:272–80. https://doi.org/10.1002/app.
[46] Gogolewski S, Pennings AJ. Resorbable materials of poly (l-lactide). II. Fibers spun from solutions of poly (l-lactide) in good solvents. J Appl Polym Sci 1983;28:1045–61.
[47] Tomé LC, Pinto RJB, Trovatti E, Freire CSR, Silvestre AJD, Neto CP, et al. Transparent bionanocomposites with improved properties prepared from acetylated bacterial cellulose and poly(lactic acid) through a simple approach. Green Chem 2011;13:419–27. https://doi.org/10.1039/c0gc00545b.
[48] Yokesahachart C, Yoksan R. Effect of amphiphilic molecules on characteristics and tensile properties of thermoplastic starch and its blends with poly(lactic acid). Carbohydr Polym 2011;83:22–31. https://doi.org/10.1016/j.carbpol.2010.07.020.
[49] Huneault MA, Li H. Morphology and properties of compatibilized polylactide/thermoplastic starch blends. Polymer 2007;48:270–80. https://doi.org/10.1016/j.polymer.2006.11.023.
[50] Akrami M, Ghasemi I, Azizi H, Karrabi M, Seyedabadi M. A new approach in compatibilization of the poly(lactic acid)/thermoplastic starch (PLA/TPS) blends. Carbohydr Polym 2016;144:254–62. https://doi.org/10.1016/j.carbpol.2016.02.035.
[51] Masina N, Choonara YE, Kumar P, du Toit LC, Govender M, Indermun S, et al. A review of the chemical modification techniques of starch. Carbohydr Polym 2017;157:1226–36. https://doi.org/10.1016/j.carbpol.2016.09.094.
[52] Noivoil N, Yoksan R. Oligo(lactic acid)-grafted starch: a compatibilizer for poly(lactic acid)/thermoplastic starch blend. Int J Biol Macromol 2020;160:506–17. https://doi.org/10.1016/j.ijbiomac.2020.05.178.
[53] Solarski S, Ferreira M, Devaux E. Characterization of the thermal properties of PLA fibers by modulated differential scanning calorimetry. Polymer 2005;46:11187–92. https://doi.org/10.1016/j.polymer.2005.10.027.
[54] Drieskens M, Peeters R, Mullens J, Franco D, Lemstra PJ, Hristova-Bogaerds DG. Structure versus properties relationship pf poly(lactic acid). I. Effect of crystallinity on barrier properties. J Polym Sci, Part B: Polym Phys 2009;47:2247–58. https://doi.org/10.1002/polb.
[55] Ferri JM, Garcia-Garcia D, Carbonell-Verdu A, Fenollar O, Balart R. Poly(lactic acid) formulations with improved toughness by physical blending with thermoplastic starch. J Appl Polym Sci 2018;135:1–8. https://doi.org/10.1002/app.45751.
[56] Androsch R, Schick C, Di Lorenzo ML. Melting of conformationally disordered crystals (α′ phase) of poly(l -lactic acid). Macromol Chem Phys 2014;215:1134–9. https://doi.org/10.1002/macp.201400126.
[57] Kawai T, Rahman N, Matsuba G, Nishida K, Kanaya T, Nakano M, et al. Crystallization and melting behavior of poly (L-lactic acid). Macromolecules 2007;40:9463–9. https://doi.org/10.1021/ma070082c.
[58] Pan P, Zhu B, Kai W, Dong T, Inoue Y. Polymorphic transition in disordered poly(L-lactide) crystals induced by annealing at elevated temperatures. Macromolecules 2008;41:4296–304. https://doi.org/10.1021/ma800343g.
[59] Thomason JL. The influence of fibre properties on the properties of glass-fibre-reinforced polyamide 6,6. J Compos Mater 2000;34:158–72.
[60] Keener TJ, Stuart RK, Brown TK. Maleated coupling agents for natural fibre composites. In: Compos. Part A Appl. Sci. Manuf., vol. 35. Elsevier; 2004. p. 357–62. https://doi.org/10.1016/j.compositesa.2003.09.014.
[61] Sanadi AR, Caulfield DF, Jacobson RE, Rowell RM. Renewable agricultural fibers as reinforcing fillers in plastics: prediction of thermal properties. J Therm Anal Calorim 2009;96:85–90. https://doi.org/10.1007/s10973-008-9855-8.
[62] Doan TTL, Gao SL, Mäder E. Jute/polypropylene composites I. Effect of matrix modification. Compos Sci Technol 2006;66:952–63. https://doi.org/10.1016/j.compscitech.2005.08.009.
[63] Teramoto Y. Recent advances in multi-scale experimental analysis to assess the role of compatibilizers in cellulosic filler-reinforced plastic composites. 2021.
[64] Kakou CA, Arrakhiz FZ, Trokourey A, Bouhfid R, Qaiss A, Rodrigue D. Influence of coupling agent content on the properties of high density polyethylene composites reinforced with oil palm fibers. Mater Des 2014;63:641–9. https://doi.org/10.1016/j.matdes.2014.06.044.
[65] Sanadi AR, Young RA, Clemons C, Rowell RM. Recycled newspaper fibers as reinforcing fillers in thermoplastics: Part I-analysis of tensile and impact properties in polypropylene. J Reinforc Plast Compos 1994;13:54–67. https://doi.org/10.1177/073168449401300104.
[66] Fu S-Y, Lauke B. Effects of fiber length and fiber orientation distributions on the tensile strength of short-fiber-reinforced polymers. Compos Sci Technol 1996;56:1179–90.
[67] Espinach FX, Julian F, Verdaguer N, Torres L, Pelach MA, Vilaseca F, et al. Analysis of tensile and flexural modulus in hemp strands/polypropylene composites. Compos B Eng 2013;47:339–43. https://doi.org/10.1016/J.COMPOSITESB.2012.11.021.
[68] Tarrés Q, Oliver-Ortega H, Espinach FX, Mutjé P, Delgado-Aguilar M, Méndez JA. Determination of mean intrinsic flexural strength and coupling factor of natural fiber reinforcement in polylactic acid biocomposites. Polymers 2019;11. https://doi.org/10.3390/polym11111736.
[69] Alves Fidelis ME, Pereira TVC, Gomes ODFM, De Andrade Silva F, Toledo Filho RD. The effect of fiber morphology on the tensile strength of natural fibers. J Mater Res Technol 2013;2:149–57. https://doi.org/10.1016/j.jmrt.2013.02.003.
[70] Rao KMM, Rao KM. Extraction and tensile properties of natural fibers: vakka, date and bamboo. Compos Struct 2007;77:288–95. https://doi.org/10.1016/j.compstruct.2005.07.023.
[71] Ku H, Wang H, Pattarachaiyakoop N, Trada M. A review on the tensile properties of natural fiber reinforced polymer composites. Compos B Eng 2011;42:856–73. https://doi.org/10.1016/j.compositesb.2011.01.010.
[72] Hirsch TJ. Modulus of elasticity of concrete affected by elastic moduli of cement paste matrix and aggregate. J Proc 1962;59:427–52.
[73] Neagu RC, Gamstedt EK, Berthold F. Stiffness contribution of various wood fibers to composite materials. J Compos Mater 2006;40:663–99. https://doi.org/10.1177/0021998305055276.
[74] Warlin N, Garcia Gonzalez MN, Mankar S, Valsange NG, Sayed M, Pyo SH, et al. A rigid spirocyclic diol from fructose-based 5-hydroxymethylfurfural: synthesis, life-cycle assessment, and polymerization for renewable polyesters and poly(urethane-urea)s. Green Chem 2019;21:6667–84. https://doi.org/10.1039/c9gc03055g.
[75] Yuan Y, Guo M. Do green wooden composites using lignin-based binder have environmentally benign alternatives? A preliminary LCA case study in China. Int J Life Cycle Assess 2017;22:1318–26. https://doi.org/10.1007/s11367-016-1235-1.
[76] Walker S, Rothman R. Life cycle assessment of bio-based and fossil-based plastic: a review. J Clean Prod 2020;261:121158. https://doi.org/10.1016/j.jclepro.2020.121158.
[77] Innocenti FD, Razza F, Fieschi M, Bastioli C, Fieschi S, Donizetti VG. Life cycle management in bioplastics production. 1989.
[78] Lopes E, Dias A, Arroja L, Capela I, Pereira F. Application of life cycle assessment to the Portuguese pulp and paper industry. J Clean Prod 2002;11:51–9. https://doi.org/10.1016/S0959-6526(02)00005-7.